Reactor Fault Diagnosis Based on CNN-LSTM Hybrid Neural Network

Xiangdong Li*, Hui Dan, Chunsheng Wang, Liuxin Nie
Jiaozuo Guangyuan Electric Power Group Co., Ltd, Jiaozuo, Henan, China
**Corresponding Author.*

Abstract: The acoustic signals generated by electrical insulation defects and mechanical failures during the operation of dry reactor contain a large amount of equipment state information, which can be used as an important feature parameter for the diagnosis of defects and failures. In view of the insufficiency of a single neural network to extract the temporal sequence features, this paper proposes a reactor fault diagnosis algorithm based on CNN-LSTM network, using CNN to mine the local spatial feature information of the spectrogram, and LSTM to mine the temporal sequence information of the spectrogram. Physical experimental platforms for electrical insulation defects and mechanical faults in reactors were established. Three fault samples were created for each fault type, and acoustic wave data and acoustic signals were collected during the evolution of insulation defects and mechanical faults in dry-type reactors. Experiments show that the method in this paper significantly improves the feature mining ability of the spectrogram, and effectively improves the fault diagnosis accuracy.

Keywords: Reactor; Acoustic Signal; Spectrogram Feature Extraction; Neural Network; Fault Diagnosis

1. Introduction

Dry-type reactors are indispensable components of modern power systems, providing essential functionalities such as voltage stabilization, power factor correction, and harmonic filtering. Unlike oil-immersed reactors, dry-type reactors are favored for their safety, environmental friendliness, and low maintenance requirements. However, due to the harsh operating environments—characterized by long-term vibration, high temperatures, and electrical stress—dry-type reactors are prone to developing faults such as insulation defects and mechanical failures. These faults can lead to unplanned shutdowns, reduced operational efficiency, and significant economic losses[1,2]. Ensuring the reliability of these reactors is, therefore, of paramount importance for maintaining the safety and stability of power grids.

The ability to quickly and accurately identify the type and severity of faults in dry-type reactors is critical for minimizing downtime and avoiding costly repairs. Current fault diagnosis methods have achieved notable success in identifying mechanical issues such as core deformation and loose bolts. However, challenges remain in diagnosing electrical faults, such as insulation degradation and partial discharges, which play a major role in the long-term reliability of reactors[3]. Addressing these challenges requires innovative approaches that can simultaneously handle mechanical and electrical faults in real-time.

Fault diagnosis methods based on vibration signal analysis are among the most widely used approaches for reactor and transformer monitoring. Vibration signals are highly sensitive to mechanical changes, making them effective for detecting structural issues such as mechanical loosening and deformation[4,6]. However, these methods often fail to capture electrical fault characteristics, such as those arising from insulation defects. This gap in diagnostic capability highlights the need for more comprehensive monitoring approaches that can address both mechanical and electrical fault types. Additionally, existing vibration-based research primarily focuses on assessing the severity of mechanical loosening, offering limited insight into fault evolution or the interactions between multiple fault types.

To overcome these limitations, acoustic signal-based fault diagnosis has emerged as a promising alternative. Acoustic signals,

generated by both mechanical and electrical faults, provide a rich source of information about the internal condition of the reactor. Insulation defects, for example, often produce partial discharge sounds, while mechanical faults generate vibrations that propagate as acoustic waves. Acoustic signal analysis offers several advantages, including non-invasiveness, high sensitivity, and the ability to capture both mechanical and electrical fault information in real-time. These advantages make acoustic-based diagnosis particularly well-suited for the demands of modern power systems.

The growing adoption of AI techniques in fault diagnosis has further expanded the potential of acoustic signal analysis. Deep learning, in particular, has revolutionized various fields, including computer vision, speech recognition, and fault detection. By leveraging powerful neural network architectures, researchers can analyze complex patterns in high-dimensional data, making deep learning an ideal choice for diagnosing faults in reactors[7,8]. One of the most promising approaches in this area involves transforming one-dimensional time-series signals, such as acoustic or vibration signals, into two-dimensional image representations. This transformation enables the application of Convolutional Neural Networks (CNNs), which excel at extracting spatial features from image data.

Several studies have demonstrated the effectiveness of CNNs in fault diagnosis. For instance, literature Gu et al,. used grey-scale spectrograms of time-frequency domain data as input for the LeNet network to identify faults. Similarly [9], Gao Shuguo et al employed data augmentation techniques to enhance grey-scale images[10], improving the robustness of CNN-based diagnostic models. While these methods achieved encouraging results, they also introduced challenges. The conversion of time-frequency data into grey-scale images often results in the loss of critical fault-related information, reducing diagnostic accuracy in complex fault scenarios. To address this issue, advanced techniques such as Recurrence Plot (RP) encoding have been proposed, enabling more detailed representations of fault signals for CNN-based analysis[11]. Additionally, Cui Guiyan et al used Gram angle fields and AlexNet to diagnose transformer winding loosening[12], demonstrating the potential of alternative image-based representations. However, many of these studies lack comparative evaluations of different methods and architectures, limiting their applicability to diverse operational conditions.

Acoustic signals often possess time-varying characteristics, such as changes in amplitude, frequency, and phase over time. These temporal variations are key to understanding fault progression and distinguishing between different types of faults. While CNNs are proficient at extracting spatial features from data, they struggle to capture sequential or temporal relationships. In contrast, Long Short-Term Memory (LSTM) networks are highly effective for handling sequential data, as they can model both short-term and long-term dependencies in time-series information. By integrating CNNs for spatial feature extraction and LSTMs for capturing temporal dynamics, a hybrid model can be created to effectively address the shortcomings of each individual method and provide a more comprehensive solution for fault diagnosis in time-series data.

In this study, we propose a novel fault diagnosis algorithm based on a CNN-LSTM hybrid network. This approach integrates the strengths of CNNs and LSTMs to provide a comprehensive solution for diagnosing faults in dry-type reactors. Specifically, the CNN component is used to extract local spatial features from acoustic signal spectra, while the LSTM component captures temporal sequence information. By fusing spatial and temporal features, the proposed model aims to enhance diagnostic accuracy and efficiency. The proposed algorithm is evaluated using a combination of experimental and simulated data to ensure its robustness and applicability. The study also includes a comparative analysis of different diagnostic methods and network architectures to validate the effectiveness of the CNN-LSTM hybrid approach.

2. Methods

2.1 CNN and LSTM

CNN which is shown in Figure 1 can obtain multiple feature parameters for diagnosis, which helps to improve the diagnosis accuracy. CNNs are highly effective in processing and classifying input data. However, they are limited to analyzing individual inputs

independently and lack the ability to capture temporal dependencies across inputs. For instance, when failure feature maps from a developmental process are used as input, CNNs cannot effectively extract the temporal characteristics between different maps. LSTM networks, by contrast, are a type of RNN enhanced with gating mechanisms. These gates include the forget gate, input gate, and output gate. The unfolded structure of an LSTM is illustrated in Figure 2.

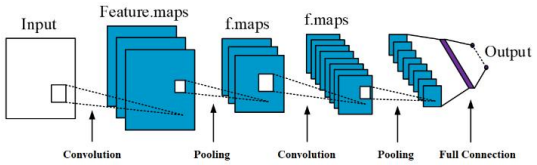

Figure 1. Typical Convolutional Neural Network

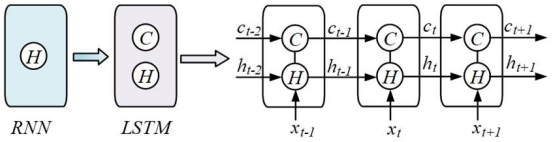

Figure 2. The Unfolding Structure of LSTM

2.2 CNN-LSTM Hybrid Networks

CNN-LSTM is a combination of CNN and LSTM, which integrates the advantages of the two. The spatial features of the spectrogram of the collected data (pulsed currents and acoustic signals) of the dry reactor are extracted by using the advantages of CNN that is good at extracting local features of the network inputs, and the temporal features on the spectrogram at different moments are extracted by using the advantages of LSTM that is good at extracting temporal features between different moments of inputs, and finally the pattern recognition diagnosis is carried out by a Softmax Finally, a Softmax classifier is used to diagnose the pattern recognition. Figure 3 shows the architecture of the hybrid CNN-LSTM network for pattern recognition.

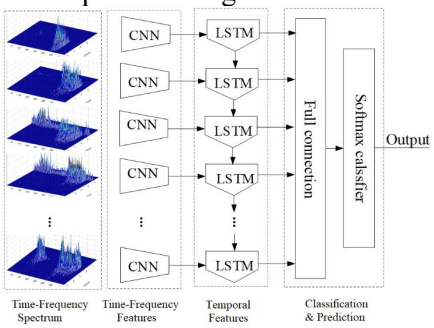

Figure 3. CNN-LSTM Hybrid Network Architecture for Spectrum Recognition

At the CNN processing layer, what needs to be extracted is the spatial information of the input atlas and the corresponding feature vectors are generated. Let N be the number of input acoustic atlases, for an input single atlas, assume that the pixel matrix of the atlas is $m \times n$, the size of the convolution kernel is $k \times k$, the periphery of the input image is filled with zero elements. Let v_{ij} is the expanded input image pixel values at (i, j) , then the elements of the window for the convolution kernel field taking v_{ij} as the top corner are

$$X_{ij} = \begin{pmatrix} v_{ij} & \cdots & v_{i(j+k-1)} \\ \vdots & \ddots & \vdots \\ v_{(i+k-1)(j)} & \cdots & v_{(i+k-1)(j+k-1)} \end{pmatrix} \tag{1}$$

After completing the convolution operation on the input spectrogram, the output of the convolutional layer Y_{ij} is performed pooling using the maximum pooling method to obtain the largest eigenvalue within the pooling window, achieve the secondary optimisation of the feature set. R_n indicates the $n-$th feature spectrogram after convolution and pooling of the input spectrogram, hen there exists,

$$V_n = \max(Y_{ij}) \tag{2}$$

When the feature extraction of all input spectrogram is completed, the feature matrix extracted by the convolutional neural network layer processing is,

$$V = (V_1, V_2, \ldots, V_N) \tag{3}$$

Since the input set of spectrogram is a set of spectrogram that fluctuate to some extent over time, assuming that the $n-$th spectrogram corresponding the time t , then it is possible to take V_n as the inputs of LSTM network at t , using V_t to indicate that V_n ,then the unit update process of the corresponding LSTM network is as follows.

$$f_t = \sigma(W_f \cdot [V_t \cdot x_t] + s_f) \tag{4}$$

$$i_t = \sigma(W_i \cdot [V_t \cdot x_t] + s_i) \tag{5}$$

$$o_t = \sigma(W_o \cdot [V_t \cdot x_t] + s_0) \tag{6}$$

$$C_t = \tanh(W_c \cdot [V_t, x_t] + s_c) \tag{7}$$

$$c_t = f_t \otimes c_{t-1} + i_t \otimes C_t \tag{8}$$

$$h_t = o_t \otimes \tanh(c_t) \tag{9}$$

where. W_f , W_i , W_o respond the weight

matrices of the forgetting, input and output gate, respectively. s_f , s_i and s_0 respond the bias terms of the respective gates. C_t is the state of the input unit, W_c , s_c are the weight matrix and the bias term of the input cell state.

3. Experiments and Analysis of Results

3.1 Testbed Construction and Fault Setting

The main equipment used in this experiment are: dry-type air-core reactors with a rated voltage of 10kV;power-frequency transformers with a capacity of 50 kVA, a primary voltage of 0.4 kV, and a secondary voltage of 100 kV; capacitive voltage dividers with a rated voltage of 100 kV, a voltage division ratio of 1000:1, and a capacitance value of 415.1 pF; current - limiting resistors with a resistance value of 4 kΩ; high-current generators with an input voltage of 380 V, an output of 63.5 V, an input current of 44 A, and an output rated current of 262.4 A. The filter used in the experiment is a low - pass filter. Its operating frequency is 0-20 kHz. High-frequency noise above 20 kHz will be suppressed, and environmental noise below 100 Hz will be directly filtered out by the program during data processing. The maximum rated current of the circuit - breaker in the laboratory is 100 A, which meets the requirements of the laboratory. The experimental principle and platform construction are shown in Figure 4.

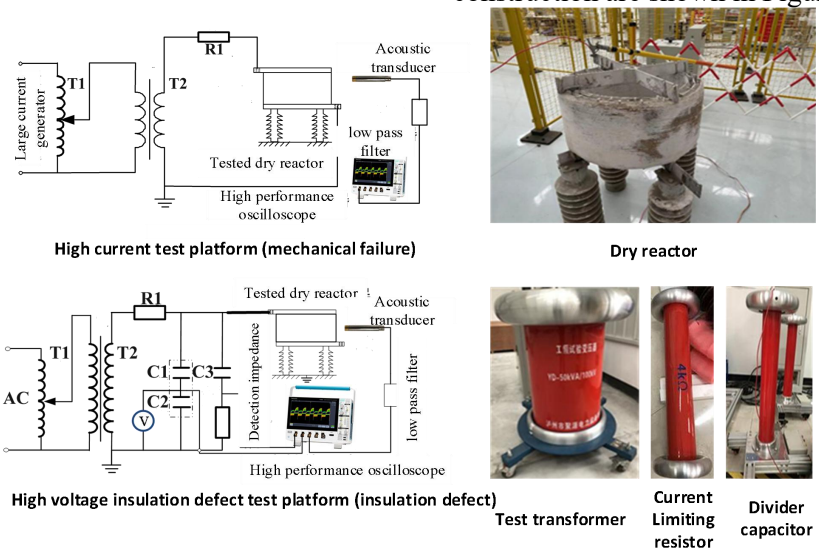

Figure 4. Experimental Principle and Platform Construction

Metal foreign matter and insulation pollution defects were set on the 10kV dry reactor, as shown in Fig. 5(a) and Fig. 5(b), respectively. Metallic foreign matter is simulated by adsorbing multiple copper wires of different lengths on the dry reactor package, and dirt is coated by 36.4 mg of diatomaceous earth mixed with 5.2 mg of NaCl in unit cm 2 in a 7:1 ratio.

The dry reactor is affected by electromagnetic force during operation, which leads to the loosening of bolts. The test simulates the bolt loosening fault by adjusting the preload of bolts, as shown in Fig. 5(c). According to the mechanical structure of the dry reactor, the test simulates the support insulator loosening faults by simultaneously loosening the fixing bolts of several support insulators on the lower star frame, as shown in Fig. 5(d).

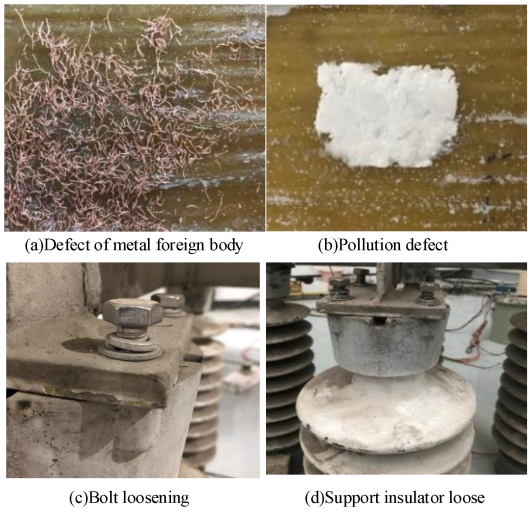

Figure 5. Fault Setting

3.2 Training Performance

We introduced a Max-Pooling layer after the

CNN module to reduce the dimensionality of feature vectors, which also helps decrease the computational load of the network. Following the Max-Pooling layer, an LSTM module with 64 LSTM units is added, incorporating a Dropout layer with a rate of 0.2 for regularization to mitigate the risk of overfitting. The training process of the CNN-LSTM hybrid network involves both forward propagation and backward propagation, where the gradient descent algorithm is used during the backward phase. The training steps are outlined as follows:

(1) Network Initialization: This step consists of two components. Input Standardization: For input feature maps, the data must be standardized into pixel matrices compatible with the convolutional neural network. Parameter Configuration: The structural parameters of the network are set, including network weights, convolution kernel size, stride size, pooling window size, pooling method, learning rate, and the number of training iterations.

(2) Forward Propagation: Calculate the network's output and determine the error between the output and the target value.

(3) Backward Propagation: If the error exceeds the desired threshold, gradient descent is applied to update the network's weights. If the error is already within the acceptable range, there is no need for backpropagation, and the training process concludes.

(4) Training Completion: Repeat the process until the error between the network output and the target value meets the expected threshold, signaling the end of training.

In order to verify that the CNN-LSTM network has better diagnostic performance, it is compared and analysed with the CNN and LSTM, and the training process is shown in Figure 6, which reveals that our proposed network has better diagnostic performance, faster convergence speed and better robustness.

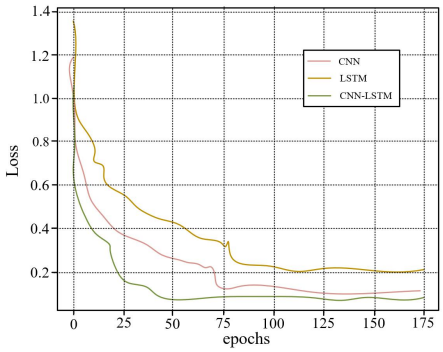

Figure 6. Visualisation of the Training Process

3.3 Results of Fault Diagnosis

The diagnostic targets are three types of typical insulation defects and three types of typical mechanical faults in dry-type reactors: metal protrusion defects, surface pollution defects, metal foreign object defects, bolt loosening, support insulator cracks, and support insulator loosening. The input data consists of multi-source feature spectrograms of faults, with the ratio of 8:2 between the training set and test set. The network consists of 5 convolutional layers, 5 pooling layers, and 1 LSTM layer, with all other parameters set to system defaults. The grayscale-processed acoustic spectrogram single-channel matrix data is used as the input for training and diagnostic recognition.

The same spectrogram data is separately input into the CNN and LSTM. The parameter settings for CNN and LSTM are the same as those of the CNN-LSTM network. The diagnostic performance of the CNN-LSTM network, CNN network, and LSTM network for typical insulation defects and mechanical faults in dry-type reactors is compared. The comparison results are shown in Table 1.

Table 1. Comparison Results of Typical Insulation Defects and Mechanical Fault of Reactors

P_r	Metal foreign objects	Surface pollution	Metal protrusions defects	Loose bolts	Loose insulators	Cracked insulators
CNN	83%	80%	100%	94%	93%	88%
LSTM	80%	78%	98%	91%	89%	81%
CNN-LSTM	94%	90%	100%	97%	95%	94%

As shown in Table 1, for metal foreign object defects and dirt defects, the local multi-source spectrogram diagnosis effect of CNN-LSTM network is better than that of CNN network and LSTM network, but for metal protrusion defects, the diagnosis effect of CNN-LSTM network is the same as that of CNN and both of them are 100%. The advantage of LSTM network lies in the extraction of temporal feature information, so in the diagnosis of CNN-LSTM network on the type of metal protrusion defects, the LSTM network does not provide too much help, but for the metal foreign body defects and fouling defects, these

two types of defects of the discharge spectrum with the increase of the pressurisation time under the condition of constant voltage, the fluctuation of its corresponding discharge acoustic spectra is more obvious. The fluctuation of the corresponding acoustic discharge spectra is obvious, which is similar to the time-domain characterisation of the acoustic signal in the previous section. At this time, the advantage of LSTM network in extracting the temporal feature information is reflected, which improves the diagnostic accuracy of CNN network for these defects.

For mechanical faults, the diagnostic effect of CNN-LSTM is better than that of LSTM and CNN, for bolt loosening and insulator loosening faults, CNN plays a dominant role in the diagnosis, while for insulator cracking defects, the recognition effect of CNN-LSTM fusion improves significantly, and the combination of the previous time-domain features can be obtained.

4. Conclusion

In this paper, a reactor fault diagnosis algorithm based on CNN-LSTM network is proposed, which adopts CNN to mine the local spatial feature information of the ma spectrograms and LSTM to mine the temporal information of the spectrograms. The experimental results show that, using multi-source feature spectrograms as input, it compares the diagnostic performance of CNN-LSTM, CNN and LSTM networks. CNN-LSTM performs well in most cases. LSTM helps with certain defects, and CNN is dominant in some mechanical fault diagnoses.

References

[1] XIAN Richang, LU Yao, CHEN Lei, et al. Fault characteristics of an inter-turn short circuit of a dry-type air core series reactor. Power System Protection and Control, 2021, 49(18): 10-16.

[2] WEI Xu, WU Shuyu, JIANG Ning, et al. Theoretical and Experimental Analyses on High-voltage Reactor Vibration Characteristics. High Voltage Apparatus, 2019, 55(11): 66-73.

[3] YU Changting, LI Dajian, CHEN Liangyuan, et al. Transformer Fault Diagnosis Technique Based on Voiceprint and Vibration. High Voltage Apparatus, 2019, 55(11): 248-254.

[4] Lecun Y, Bottou L, Bengio Y, et al. Gradient-based learning applied to document recognition. Proceed-ings of the IEEE, 1998,86(11): 2278-2324.

[5] Krizhevsky A, Sutskever I, Hinton G E. Imagenet clas-sification with deep convolutional neural networks. Communications of the ACM, 2017, 60(6): 84-90.

[6] WU Chenfang, YANG Shixi, HUANG Haizhou, et al. An improved fault diagnosis method of rolling bearings based on Le Net-5. Journal of Vibration and Shock, 2021, 40(12): 55-61.

[7] ZHANG Long, HU Yanqing, ZHAO Lijuan, et al. Fault Diagnosis of Rolling Bearings Using Recurrence Plot Coding Technique and Residual Network. Journal of Xi'an Jiaotong University, 2023, 57(02): 110-120.

[8] XUE Jiantong, MA Hongzhong, YANG Hongsu, et al. A fault diagnosis method for transformer winding looseness based on Gramian angular field and transfer learning-AlexNet. Power System Protection and Control, 2023, 51(24): 154-163.

[9] GU Yingkui, WU Kuan, LI Cheng, et al. Rolling bearing fault diagnosis based on Gram angle field and transfer deep residual neural network. Journal of Vibration and Shock, 2022, 41(21): 228-237.

[10] GAO Shu-guo, MENG Ling-ming, ZHANG Yu-kun, et al. Fault diagnosis method for core loose of high voltage shunt reactor using vibration sensing array. Journal of Vibration Engineering, 2023, 36(03): 875-884.

[11] SHAO Haidong, XIAO Yiming, YAN Shen, et al. Simulation Data-driven Enhanced Unsupervised Domain Adaptation for Bearing Fault Diagnosis. Journal of Mechanical Engineering, 2023, 59(03): 76-85.

[12] CUI Guiyan, ZHONG Qianwen, ZHENG Shubin, et al. Multi-sensor fusion bearing fault diagnosis based on VMD gray level image coding and CNN. Journal of Vibration and Shock, 2023, 42(21): 316-326.

